Electronic Supplementary information

Experimental section

Materials: The $FeCl_3 \cdot 6H_2O$, urea, and $(NH_4)_2MoS_4$ were purchased from Beijing Chemical Corp (China). Pt/C (20 wt% Pt on Vulcan XC-72R), was purchased from Alfa Aesar (China) Chemicals Co. Ltd.. Carbon cloth (CC) was purchased by Hongshan District, Wuhan Instrument Surgical Instruments business, and was pretreated with HNO_3 and then cleaned by sonication in water and ethanol for several times to remove surface impurities. The ultrapure water used throughout all experiments through a Millipore system. All chemicals were used as received without further purification.

Characterization: The XRD patterns were obtained from a LabX XRD-6100 X-ray diffractometer with Cu Kα radiation (40 kV, 30 mA) of wavelength 0.154 nm (RIGAKU, Japan). The X-ray photoelectron spectroscopy (XPS) measurements were performed on an ESCALABMK II X-ray photoelectron spectrometer using Mg as the exciting source. The scanning electron microscopy (SEM) were collected from the tungsten lamp-equipped SU3500 scanning electron microscope at an accelerating voltage of 20 kV (HITACHI, Japan). The transmission electron microscopy (TEM) images were obtained from a Zeiss Libra 200FE transmission electron microscope operated at 200 kV. Surface area measurement was performed on a Micromeritics ASAP 2020surface area (Quantachrome, USA). Inductively coupled plasma mass spectrometry (ICP-MS) analysis was performed on Thermo Scientific iCAP6300.

Preparation of FeOOH NRA/CC: 2.702 mg $FeCl_3 \cdot 6H_2O$ and 0.9 g urea were dissolved in 100 mL ultrapure water under magnetic stirring to form a uniform solution. Then, the pre-treated CC and the above solution were transferred into a 50 mL Teflon-lined stainless-steel autoclave and maintained at 373 K for 4 h. After cooled to room temperature, the product was washed with ultrapure water for three times. Then the FeOOH NRA/CC was obtained.

Preparation of $FeMoS_4$ NRA/CC: The $FeMoS_4$ NRA/CC was prepared by hydrothermal reaction. In a typical synthesis, $(NH_4)_2MoS_4$ (0.03 g) was dissolved in

40 mL water under vigorous stirring for 60 min. The prepared FeOOH NRA/CC and $(NH_4)_2MoS_4$ solution were all transferred into a Teflon-lined stainless autoclave (50 mL). The reaction was conducted at 433 K for 10 h. After cooled down to room the temperature, the $FeMoS_4$ NRA/CC was taken out and washed with water thoroughly before vacuum dried.

Electrochemical measurement: The electrochemical measurements were performed on a CHI 660E electrochemical workstation (Chenhua, Shanghai). A three-electrode system was used in the experiment: a graphite rod was used as the counter electrode; a saturated calomel electrode (SCE) was used as the reference electrode and the as-prepared $FeMoS_4$ NRA/CC was used as the working electrode. All the measurements were performed at 298 K in 1 M PBS solution. The reference electrode was calibrated to the reversible hydrogen electrode (RHE): E (RHE) = E (SCE) + (0.242 + 0.059 pH) = E (SCE) + 0.655 V.

Turnover frequency (TOF) calculation: To compare the activity of $FeMoS_4$ NRA/CC with other non-noble-metal catalysts, the TOF for each active site was calculated by the equation (1):

$$TOF = jA/2Fm \quad (1)$$

Where j is current density (A cm^{-2}) at defined overpotential of the electrochemical measurement in 1 M PBS; A is the geometric area of the testing electrode; 2 indicates the mole of electrons consumed for evolving one mole H_2 from water; F is the Faradic constant (96485 C mol^{-1}); m is the number of active sites (mol), which can be extracted from the linear relationship between the oxidation peak currents and scan rates by the equation (2) [1,2]:

$$slope = n^2F^2A\Gamma_0/4RT \quad (2)$$

where n is the numbers of electron transferred; $m = A\Gamma_0$; Γ_0 is the surface concentration of active sites (mol cm^{-2}); R and T are the ideal gas constant and the absolute temperature, respectively.

FE determination: The FE was calculated by comparing the amount of measured H_2 generated by cathodal electrolysis with calculated H_2 (assuming 100% FE). GC analysis was carried out on GC–2014C (Shimadzu Co.) with thermal conductivity

detector and nitrogen carrier gas. Pressure data during electrolysis were recorded using a CEM DT-8890 Differential Air Pressure Gauge Manometer Data Logger Meter Tester with a sampling interval of 1 point per second.

Computational details: Spin-polarized density functional theory calculations were performed using the Vienna ab initio simulation package (VASP).[3–5] We used the PBE functional for the exchange-correlation energy[6] and projector augmented wave (PAW) potentials.[7,8] The kinetic energy cutoff was set to 450 eV. The ionic relaxation was performed until the force on each atom is less than 0.01 eV/Å. The k-points meshes were 3×3×1 with Monkhorst-Pack method.[9] DFT-D[4] method was used to calculate the adsorption energy, which is an efficient method to approximately account for the long-range vdW interactions.[10] The simulations performed were based on a $FeMoS_4$ model structure with 16 Fe, 16 Mo and 56 S atoms. To minimize the undesired interactions between images, a vacuum of at least 15 Å was considered along the z axis. The free energy change for H* adsorption on $FeMoS_4$ and FeOOH surfaces (ΔG_H) was calculated as follows, which is proposed by Norskov and oworkers[11]:

$$\Delta G_H = E_{total} - E_{sur} - E_H^2/2 + \Delta E_{ZPE} - T\Delta S$$

where E_{total} is the total energy for the adsorption state, E_{sur} is the energy of pure surface, E_H^2 is the energy of H_2 in gas phase, ΔE_{ZPE} is the zero-point energy change and ΔS is the entropy change.

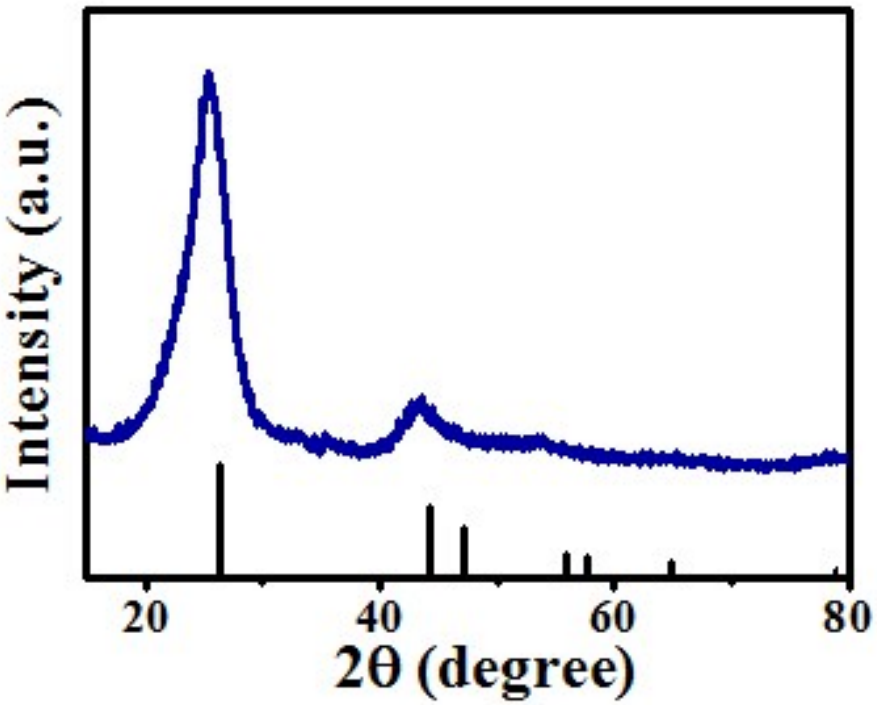

Fig. S1. XRD pattern of bare CC.

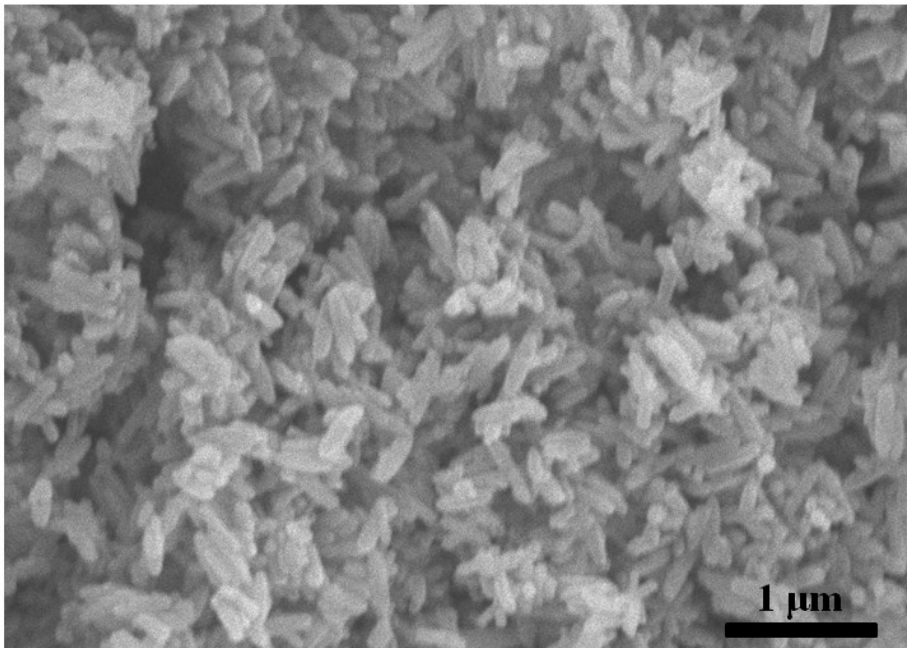

Fig. S2. SEM image of $FeMoS_4$ nanorods synthesized without CC.

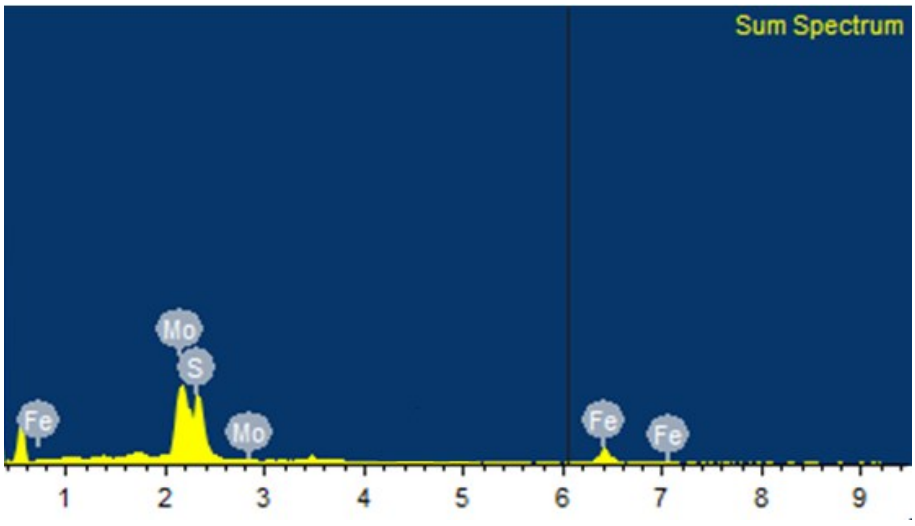

Fig. S3. EDX spectrum of $FeMoS_4$ NRA/CC.

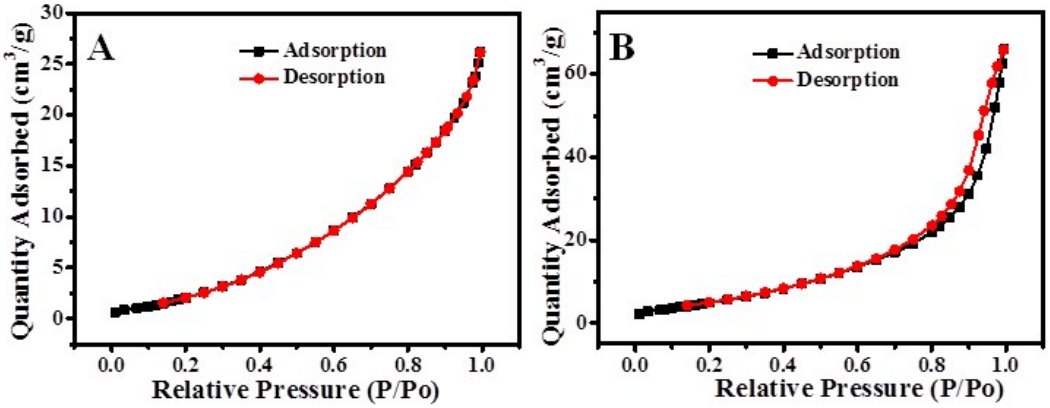

Fig. S4. Nitrogen adsorption/desorption curves of (A) FeOOH and (B) $FeMoS_4$.

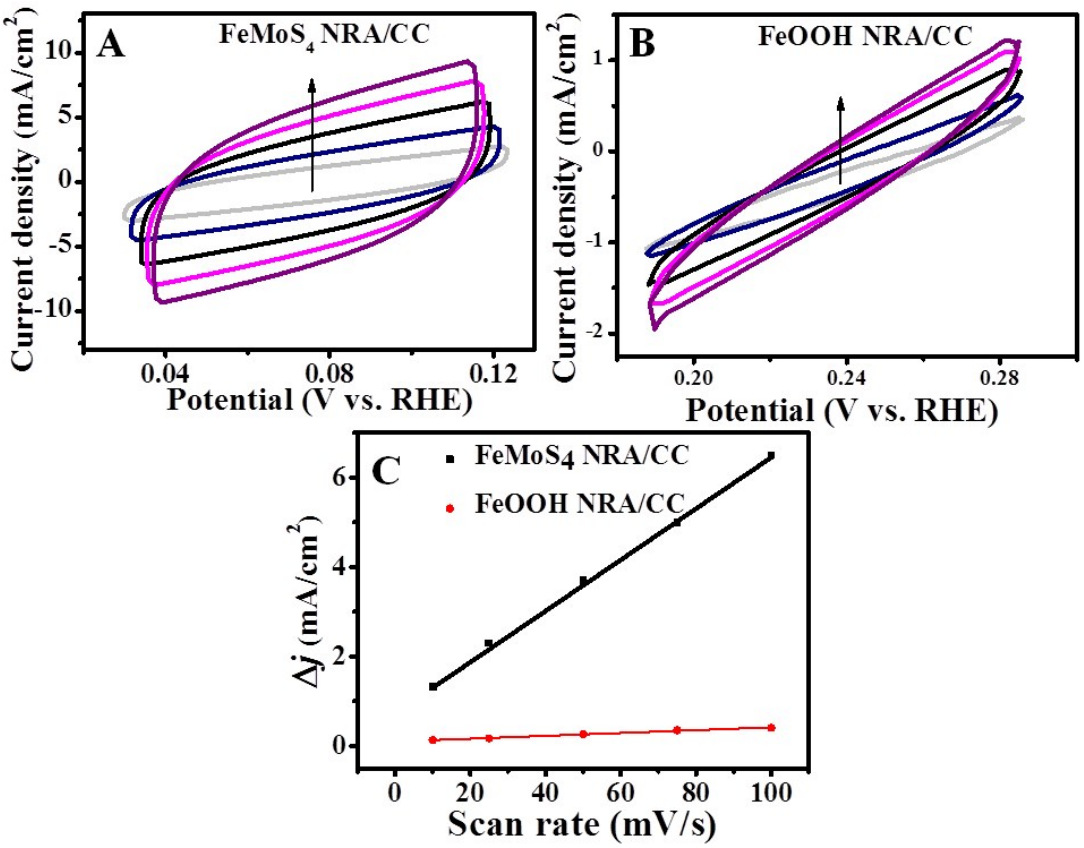

Fig. S5. CVs for (A) $FeMoS_4$ NRA/CC and (B) FeOOH NRA/CC at different scan rates. (C) Capacitive current as a function of scan rate for FeOOH NRA/CC and $FeMoS_4$ NRA/CC.

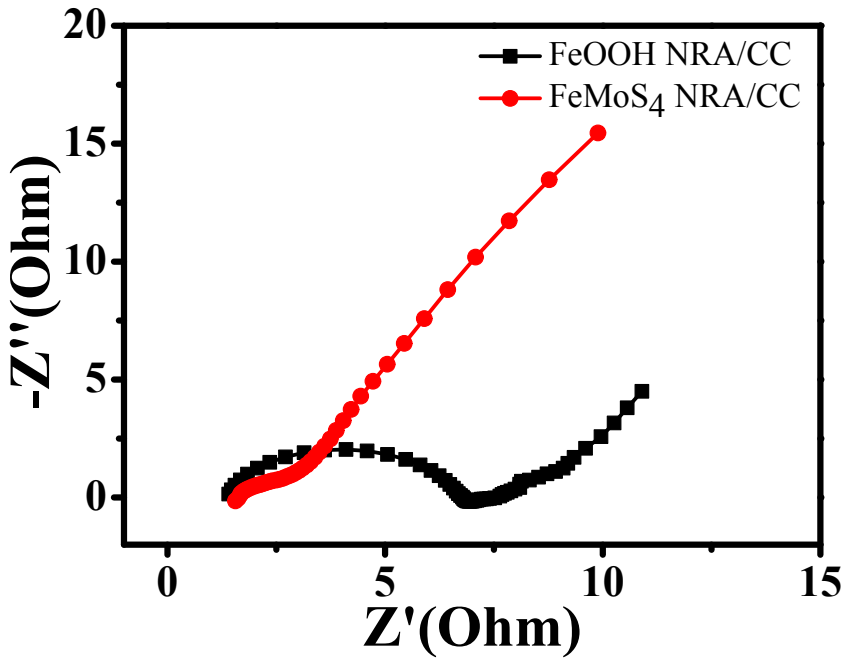

Fig. S6. EIS spectra of FeOOH NRA/CC and $FeMoS_4$ NRA/CC.

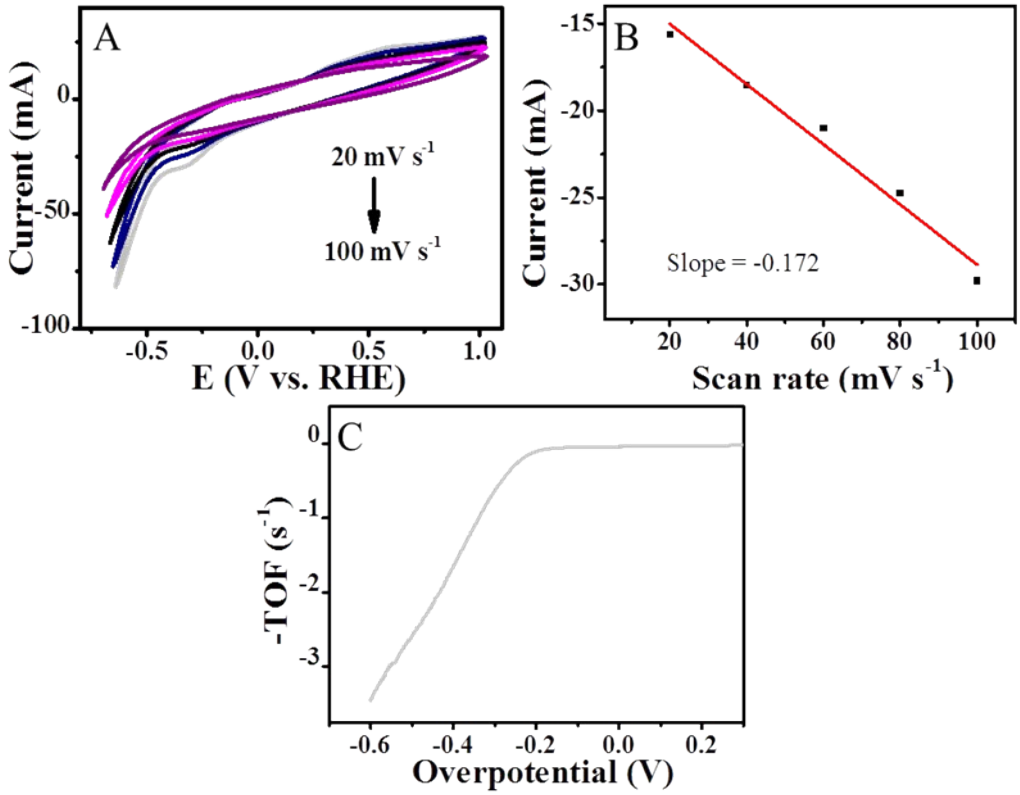

Fig. S7. (A) CVs of the $FeMoS_4$ NRA/CC at different scan rates in 1 M PBS. (B) Reduction peak current versus scan rate plot for $FeMoS_4$ NRA/CC. (C) The relationship between TOF and overpotential.

Table S1. Comparison of HER performance for $FeMoS_4$ NRA/CC with other non-noble-metal electrocatalysts at neutral pH.

Catalyst	loading (mg cm^{-2})	j (mA cm^{-2})	η (mV)	Electrolyte	Reference
$FeMoS_4$ NRA/CC	1.83	10	204	1.0 M PBS	This work
$CoO/CoSe_2$/Ti	2.0	10	337	0.5 M PBS	12
WP_2 nanorods/GCE	-	10	298	1.0 M PBS	13
$CoMoS_4$/GCE	0.262	10	~ 420	1.0 M PBS	14
Co-MoS_3/GC	2.6	1	200	1.0 M PBS	15
Co-B pellets	-	10	251	0.5 M KPi	16
$CoMoS_3$/FTO	-	5	206	0.1 M PBS	17
MoB/CPE	2.0	5	250	1.0 M KOH	18
Co-NRCNTs/GCE	0.28	10	540	0.1 M PBS	19
H_2-CoCat/FTO	-	2	385	0.5 M KPi	20
carbon nanofiber @CoS_2/GCE	0.6-0.8	10	360	1.0 M PBS	21

References:

1 Y. Li, L. Zhang, X. Xiang, D. Yan and F. Li, *J. Mater. Chem. A*, 2014, **2**, 13250–13258.

2 S. Pintado, S. Goberna-Ferron, E. C. Escudero-Adan and J. R. Galan-Mascaros, *J. Am. Chem. Soc.*, 2013, **135**, 13270–13273.

3 G. Kresse and J. Furthmuller, *Comp. Mater. Sci.*, 1996, **6**, 15–50.

4 G. Kresse and J. Furthmuller, *Phys. Rev. B*, 1996, **54**, 11169–11186.

5 G. Kresse and J. Hafner, *Phys. Rev. B*, 1994, **49**, 14251–14269.

6 J. P. Perdew, K. Burke and M. Ernzerhof, *Phys. Rev. Lett.*, 1997, **78**, 1396–1396.

7 G. Kresse and D. Joubert, *Phys. Rev. B*, 1999, **59**, 1758–1775.

8 P. E. Blochl, *Phys. Rev. B*, 1994, **50**, 17953–17979.

9 H. J. Monkhorst and J. D. Pack, *Phys. Rev. B*, 1976, **13**, 5188–5192.

10 S. Grimme, *J. Comput. Chem.*, 2006, **27**, 1787–1799.

11 J. K. Noskov, T. Bligaard, A. Logadottir, J. R. Kitchin, J. G. Chen, S. Pandelov and U. Stimming, *J. Electrochem. Soc.*, 2005, **152**, J23–J26.

12 K. Li, J. Zhang, R. Wu, Y. Yu and B. Zhang, *Adv. Sci.*, 2016, **3**, 1500426.

13 H. Du, S. Gu, R. Liu and C. Li, *J. Power Sources*, 2015, **278**, 540–545.

14 L. Shao, X. Qian, X. Wang, H. Li, R. Yan and L. Hou, *Electrochim. Acta*, 2016, **213**, 236–243.

15 D. Merki, H. Vrubel, L. Rovelli, S. Fierro and X. Hu, *Chem. Sci.*, 2012, **3**, 2515–2525.

16 S. Gupta, N. Patel, A. Miotello and D. Kothari, *J. Power Sources*, 2015, **279**, 620–625.

17 P. D. Tran, S. Y. Chiam, P. P. Boix, Y. Ren, S. S. Pramana, J. Fize, V. Artero and J. Barber, *Energy Environ. Sci.*, 2013, **6**, 2452–2459.

18 H. Vrubel and X. Hu, *Angew. Chem., Int. Ed.*, 2012, **51**, 12703–12706.

19 X. Zou, X. Huang, A. Goswami, R. Silva, B. R. Sathe, E. Mikmeková and T. Asefa, *Angew. Chem., Int. Ed.*, 2014, **51**, 4372–4376.

20 S. Cobo, J. Heidkamp, P. A. Jacques, J. Fize, V. Fourmond, L. Guetaz, B.

Jousselme, V. Ivanova, H. Dau, S. Palacin, M. Fontecave and V. Artero, *Nat. Mater.*, 2012, **11**, 802–807.

21 H. Gu, Y. Huang, L. Zuo, W. Fan and T. Liu, *Inorg. Chem. Front.*, 2016, **3**, 1280–1288.